Int. J. of Thermodynamics
Vol. 11 (No. 4), pp. 203-211, December 2008

ISSN 1301-9724

Synthesis, Design and Operation Optimization of the Marine Energy System for a Liquefied Natural Gas Carrier

George G. Dimopoulos* and Christos A. Frangopoulos

School of Naval Architecture and Marine Engineering,
National Technical University of Athens,
Heroon Polytechniou 9, 157 73 Zografou, Greece

Abstract

The synthesis, design and operation optimization of the marine energy system for a Liquefied Natural Gas (LNG) vessel is performed in this study. A realistic problem is formulated based on a detailed thermoeconomic model of the energy system components and the production of boil-off gas from the LNG cargo, which is used as the main fuel of the system. The time varying operation requirements of the vessel are identified and the problem is solved in a time dependent form. A novel optimization algorithm is used based on social and evolutionary metaphors. The results indicate that the duration of the trip (route) of the vessel has a significant effect on the optimum synthesis of the system.

Keywords: *Synthesis Optimization, Marine Energy Systems, Particle Swarm Optimization*

1. INTRODUCTION

Many studies of LNG propulsion systems in the literature focus on the techno-economic evaluation of predetermined configurations (Andrianos, 2006; Levander and Hannula, 2004; MAN-B&W, 2004). The objective of the present study is to propose a method for system optimization with respect to synthesis of components, their design characteristics and the operation mode during the mission of the vessel.

2. LNG MARINE ENERGY SYSTEM OPTIMIZATION

The optimization of the integrated energy system of a LNG vessel has been considered. The generic model developed and described in detail in an accompanying paper (Dimopoulos and Frangopoulos, 2008b) has been used for the synthesis, design and operation optimization of the energy system.

The optimization problem is formulated using a generic configuration (Fig. 1 in (Dimopoulos and Frangopoulos, 2008b)). The types of components and the optimization independent variables are as follows:

- High power output gas turbines (type A); the number of units (N_{GTA}) is a synthesis optimization independent variable and the common nominal output $\dot{W}_{GT_n,A}$ is a design optimization independent variable.
- Moderate power output gas turbines (type B); the number of units (N_{GTB}) is a synthesis optimization independent variable and the common nominal output $\dot{W}_{GT_n,B}$ is a design optimization independent variable.
- HRSG units; the possible connection types between gas turbines (GTs) and HRSG is a synthesis optimization independent variable ($I_{CONNECT}$). HRSG units can be either single or dual pressure with the type being a synthesis optimization independent variable (I_{HRSG}, where $I_{HRSG} = 1$ denotes a dual pressure HRSG and $I_{HRSG} = 0$ denotes a single pressure HRSG). In addition, the quality of the high pressure (HP) superheated steam varies by means of two design optimization independent variables: P_{HP} and T_{HP}. $I_{CONNECT}$ has four possible values representing types of connections:
  - $I_{CONNECT} = 0$: all gas turbines are connected to one HRSG unit.
  - $I_{CONNECT} = 1$: each gas turbine is connected to its own HRSG unit.
  - $I_{CONNECT} = 2$: a pair of one type A and one type B gas turbine is connected to a HRSG unit.
  - $I_{CONNECT} = 3$: all type A gas turbines are connected to one HRSG unit and all type B gas turbines (if present) are connected to another HRSG unit.

* Corresponding author: Phone: +30-210-7721114, Fax: +30-210-7721117, E-mail:gdimop@lme.ntua.gr

- A steam turbine driven by high pressure steam with its existence in the system being a synthesis optimization independent variable (I_{ST}).

In addition to the aforementioned, the service speed of the vessel (V_S) is a design optimization independent variable.

The system has the following operating features:

- The load of each GT can be varied independently, with the load factor of each unit ($f_{L,GT}$) being an operation optimization independent variable.
- There is an exhaust gas by-pass in each HRSG that can regulate the amount of exhaust gases supplied to the unit. The fraction of the exhaust gas flow rate passing through the HRSG is an operation optimization independent variable (f_{bp}).
- When a dual pressure boiler is present in the configuration, the fraction of the total steam supplied as LP steam (f_{LP}) can be varied by means of a regulating valve and it is an operation optimization independent variable.
- There is a throttling valve between the HP and LP steam lines. The fraction of HP steam throttled to LP (f_{thr}) is an operation optimization independent variable.
- The steam turbine has an extraction point to supply LP steam. The fraction of the extracted mass flow rate (f_{ext}) is an operation optimization independent variable.

The generic COGES system and the single and dual pressure HRSGs are depicted in Figs. 1 and 2 of the accompanying paper (Dimopoulos and Frangopoulos, 2008b). All optimization independent variables are denoted in these figures.

The detailed boil-off gas production model developed in Dimopoulos and Frangopoulos (2008a) is used for the system operation simulation. The fact that both the quantity and the thermodynamic properties of BOG vary during voyage is taken into consideration in the model. This variability combined with the consideration of five different operating modes of the vessel, makes the operation optimization problem highly time dependent, as it is described in detail in Section 3.

3. PROBLEM FORMULATION

3.1 Statement of the optimization problem

The maximization of the Net Present Value (NPV) of the investment has been selected as the optimization objective function:

$$\max_{\mathbf{w},\mathbf{z},\mathbf{x}} \mathrm{NPV} = -C_C + \sum_{y=1}^{N_e} \frac{F_y}{(1+i_r)^y} \tag{1}$$

where **w, z** and **x** are the set of synthesis, design and operation optimization independent variables, respectively:

$$\mathbf{w} = \left\{ N_{GTA}, N_{GTB}, I_{CONNECT}, I_{HRSG}, I_{ST} \right\}$$

$$\mathbf{z} = \left\{ \dot{W}_{GT_n,A}, \dot{W}_{GT_n,B}, V_S, \Delta P_{HP}, \Delta T_{HP} \right\} \tag{2}$$

$$\mathbf{x} = \left\{ f_{LGT_{i,t}}, f_{bp_{j,t}}, f_{LP,t}, f_{thr,t}, f_{ext,t} \right\}_{\substack{t=1,\ldots,N_T \\ i=1,\ldots,N_{GTA} \\ j=1,\ldots,N_{HRSG}}}$$

It is noted that the variable f_{LP} appears in the problem only when a dual pressure HRSG is present in the configuration ($I_{BOILER} = 1$).

The optimization problem is subject to energy demand constraints:

$$g_{1t} = \dot{W}_{P_{R_t}} - \dot{W}_{D_t} = 0 \ , \ t=1,\ldots,N_T \tag{3}$$

$$g_{2t} = \dot{m}_{LP_{Pr,t}} - \dot{m}_{LP_{D,t}} = 0 \ , \ t=1,\ldots,N_T \tag{4}$$

design constraints:

$$g_3 = \dot{W}_{ST_n} - \dot{W}_{ST_{UB}} \le 0 \tag{5}$$

and logical constraints:

$$g_4 : \ \text{if} \ \underset{\text{(ST not present)}}{I_{ST} = 0} \ \text{then} \begin{cases} f_{thr} = 1 \\ f_{ext} = 0 \end{cases} \tag{6}$$

$$g_5 : \ \text{if} \ \underset{\text{(no Level B GTs)}}{N_{GTB} = 0} \ \text{then} \ I_{CONNECT} = 0 \text{ or } 1 \tag{7}$$

In addition, all the design and operation optimization independent variables are bounded by technical upper and lower limits.

The capital cost of the system appearing in Eq. (1) is the sum of individual equipment purchase costs multiplied by an installation cost factor:

$$C_C = \left(\sum_{i=1}^{N_{GT}} C_{C_{GT}} + \sum_{i=1}^{N_{HRSG}} C_{C_{HRSG}} + I_{ST} \cdot C_{C_{ST}} \right) \cdot \phi \tag{8}$$

where

$$N_{GT} = N_{GTA} + N_{GTB} \tag{9}$$

$$N_{HRSG} = f\left(I_{CONNECT}, N_{GTB}, N_{GTA}\right) \tag{10}$$

The cost functions appearing in Eq. (8) are given in (Dimopoulos and Frangopoulos, 2008b).

The profit (net cash flow) in a round trip of the vessel is determined as the difference between the income generated by delivering a quantity of LNG at CIF price at the import terminal and the operating expenses during voyage, which include the purchase or

production costs of LNG at FOB price in the export terminal (Dimopoulos and Frangopoulos, 2008b):

$$F_{rnd} = CIF \cdot V_{Delivered} - C_{op} \quad (11)$$

The operating expenses per round trip are:

$$C_{op,rnd} = 2 \cdot C_{port} + \left(FOB \cdot \rho_{LNG} \cdot V_{tot}\right) + \\ + \sum_{k=1}^{5} \left[C_{LNG} + C_{MGO} + C_m\right] \cdot \Delta\tau_k \quad (12)$$

The annual net cash flow F_y appearing in Eq. (1) is the sum of net cash flows of all the round-trips in a year.

The voyage profile of a LNG vessel has been decomposed in five characteristic phases:

1. Voyage in full load condition from the loading to the off-loading terminal (port).
2 Voyage in ballast condition from the off-loading to the loading terminal.
3. Manoeuvring during approach of both the loading and off-loading terminals.
4. LNG loading period in the loading terminal.
5. LNG delivery period in the off-loading terminal.

Further details are given in Dimopoulos and Frangopoulos (2008b).

Each phase of the round trip of the LNG vessel has been determined in detail in Dimopoulos and Frangopoulos (2008b). It is noted, that the duration of the full load and ballast voyages (phases 1 and 2) is a function of the vessel service speed, which is a design independent variable.

3.2 Time decomposition of the optimization problem

The solution of the optimization problem stated by Eqs. (1)-(7) is rather difficult because of the following features:

a) The variation in BOG quantity and properties during voyage, which results in a high number of time intervals with different characteristics that need to be considered.
b) The service speed of the vessel is an independent variable and thus the voyage duration depends on it. Therefore, the number of time intervals also varies with the service speed.
c) The number of operation optimization variables varies with the synthesis of the system (see Eq. (2)).
d) The fuel used in each operation interval (BOG or MGO) depends on the phase of the round trip (Dimopoulos and Frangopoulos, 2008b) and the availability of sufficient BOG.

In order to address these difficulties, a time decomposition has been applied. Two levels of optimization problems have been considered: a) a Level A problem for synthesis and design optimization, and b) a number of Level B problems for operation optimization.

An operation optimization problem has been formulated for each of the N_T operating modes. These problems are solved iteratively for each calculation step of the Level A optimization problem. Equation (1) is written for the Level A problem:

$$\max_{\mathbf{w},\mathbf{z}} \; NPV = -C_C + \sum_{y=1}^{N_e} \frac{F_y^*}{\left(1+i_r\right)^y} \quad (13)$$

subject to constraints of Eqs. (5) to (7).

The value of F_y^* results from the solution of the Level B optimization problems see Eq. (11). Each Level B optimization problem is stated by:

$$\min_{\mathbf{x}_t} \; C_{op_t} = \left[C_{LNG} + C_{MGO} + C_m\right]_t \quad \forall t \quad (14)$$

subject to constraints of Eqs. (3) and (4).

For each day of the voyage in phases 1 and 2 in a round trip, an optimization problem is solved. The duration of a voyage is a function of the service speed and sailing distance. In addition, an operation optimization problem is solved for each of the three remaining phases 3, 4 and 5.

3.3 Simulation Models

The individual thermoeconomic models of the components of the system, namely GT, HRSG and ST units, are presented in Dimopoulos and Frangopoulos (2008b). The complete thermoeconomic model of the system is capable of assessing both nominal and off-design performance of the components. Also, statistically derived equipment cost functions have been adapted for marine applications and used in the simulation model.

The BOG quantity and properties are determined using the dynamic boil-off model described in Dimopoulos and Frangopoulos (2008a). Special attention has been given to the determination of the consumed BOG quantity, which is directly related to the system fuel cost.

The BOG flow rate $\dot{m}_{GT,tot}$ used by the GT units is determined in each evaluation step as a function of the independent variables $\mathbf{x_t}$. If the natural boil-off is higher than or equal to $\dot{m}_{GT,tot}$, then BOG is used for GT fuel and any surplus is burned in a gasification unit. If the natural boil-off is lower than $\dot{m}_{GT,tot}$, then additional BOG is produced by forced boil-off to supplement it.

If BOG production, both natural and forced, is no longer sufficient to fuel the system, then operation is switched to MGO. MGO is also used

in round-trip phases 3, 4 and 5, due to safety precautions.

For the calculation of C_{LNG} appearing in Eq. (14), the value of the unit costs of LNG (c_{LNG}) is required, which is derived as follows.

In order to maximize NPV, Eq. (13), the round trip profit must be maximized:

$$\max_{\mathbf{x}}\left(F_{rnd}\right)=\max_{\mathbf{x}}\left[CIF\cdot V_{Delivered}-C_{op}\right] \quad (15)$$

As shown in Eq. (17) of the accompanying paper (Dimopoulos and Frangopoulos, 2008b), the delivered volume is:

$$V_{Delivered}=V_{tot}-V_{BOG}-V_{H} \quad (16)$$

and according to Eq. (15) of the same paper the round trip operating cost is:

$$\begin{aligned}C_{op,rnd}&=2\cdot C_{port}+\left(FOB\cdot V_{tot}\right)+\\&+\sum_{k=1}^{5}\left[C_{LNG}+C_{MGO}+C_{m}\right]\cdot\Delta\tau_{k}\end{aligned} \quad (17)$$

By rearrangement of terms of Eqs. (15) to (17), the round-trip profit is expressed:

$$\begin{aligned}F_{rnd}&=CIF\cdot\left(V_{tot}-V_{BOG}-V_{H}\right)\\&-2\cdot C_{port}-C_{F}\end{aligned} \quad (18)$$

where

$$C_{F}=\sum_{k=1}^{5}\left[C_{MGO}+C_{m}\right]\cdot\Delta\tau_{k} \quad (19)$$

Differentiating Eq. (18) with respect to the operation independent variables yields:

$$\frac{\partial F_{rnd}}{\partial\mathbf{x}}=-CIF\cdot\frac{\partial V_{BOG}}{\partial\mathbf{x}}-\frac{\partial C_{F}}{\partial\mathbf{x}} \quad (20)$$

since only V_{BOG} and C_F are operation dependent variables.

Therefore, the maximization of the round-trip profit is equivalent with the minimization of the round-trip total operating cost:

$$\begin{aligned}&\max_{\mathbf{x}}\left(F_{rnd}\right)\Leftrightarrow\\&\min_{\mathbf{x}}\sum_{k=1}^{5}\left[CIF\cdot\dot{V}_{BOG_{k}}+C_{MGO_{k}}+C_{m_{k}}\right]\cdot\Delta\tau_{k}\end{aligned} \quad (21)$$

Equations (20) and (21) indicate that the unit cost of LNG is equal to the CIF LNG price:

$$c_{LNG}=CIF \quad (22)$$

3.4 Numerical Application

As a case study, a COGES energy system of a modern LNG carrier is optimized. The vessel has a cargo capacity of 150000 m^3 of LNG. Typical principal particulars for this ship are overall length 280 m, breadth 43 m depth 27 m and design draft 12 m (Andrianos, 2006).

The needs of the LNG carrier in electrical and thermal energy at each operating mode and various design service speeds are presented in the accompanying paper Dimopoulos and Frangopoulos (2008b). Various cost parameters have been considered in this study. Fuel prices for LNG and MGO have been collected from available databases and literature data (Andrianos, 2006; BunkerWorld, 2007). Various physical and economic parameters appearing in Sections 3.1 and 3.2, as well as in the detailed description of the model in (Dimopoulos and Frangopoulos, 2008b) are presented in Table 1.

Three typical trading routes have been considered: a) from Arab gulf to Europe (Mediterranean), with a nautical distance of about 4500 nm, b) from Arab gulf to Japan, with a nautical distance of about 6500 nm, and c) from Arab gulf to the USA east coast, with a nautical distance of about 9500 nm. Route b is the most common, since Japan is the largest world importer of LNG. However, route c is the most intriguing, since it is the longest one and demands a high cost effectiveness of the system, in order to overcome the high operating costs. The three routes are depicted in Fig. 1.

Typical LNG composition at loading terminal and BOG model parameters are given in Dimopoulos and Frangopoulos (2008a).

4. OPTIMIZATION PROCEDURE

For the numerical solution of the optimization problem, a novel algorithm has been used, which is a hybrid of evolutionary and socially inspired techniques. It combines features from the Particle Swarm Optimization (PSO) (Kennedy, et al., 2001) and the Struggle Genetic Algorithm (StrGA) (Grueninger and Wallace, 1996). The algorithm is called Particle Swarm Optimization with Struggle selection (PSOStr) and it has been successfully applied to the synthesis, design and operation optimization of energy systems (Dimopoulos and Frangopoulos, 2006; Dimopoulos, et al., 2006). A detailed description of the PSOStr algorithm appears in Dimopoulos (2007) and Dimopoulos and Frangopoulos (2006).

Evolutionary and socially inspired optimization algorithms, in their basic form, are unconstrained optimization methods. In order to handle the various constraints of the optimization problem, a constraint violation penalty method has been used. The objective functions (f) of Eqs. (13) and (14) are readily modified in order to account for constraints as follows:

$$f'\left(\mathbf{x}\right)=f\left(\mathbf{x}\right)\pm r\cdot\sum_{i}\left[\max\left(0,g_{i}\left(\mathbf{x}\right)\right)\right]^{2} \quad (23)$$

TABLE 1. Economic and physical parameters of the optimization problem.

Economic Parameters
$c_{MGO} = 0.525\ \$/kg$
$CIF = 7.0\ \$/mmBTU = 0.370\ \$/kg$
$FOB = 3.5\ \$/mmBTU = 0.185\ \$/kg$
$c_{m_{GT}} = 2.5 \cdot 10^{-3}\ \$/kWh_e$
$c_{m_{HRSG}} = 5.0 \cdot 10^{-3}\ \$/kWh_{th}$
$c_{m_{ST}} = 4.0 \cdot 10^{-3}\ \$/kWh_e$
$C_{port} = 75000\ \$ / \text{port call}$
$\phi = 2.0$
$N_e = 20$ years
$i_r = 8\%$
Physical Parameters
$T_a = 305.15$ K
$H_{u,MGO} = 43100$ kJ/kg
$P_{LP} = 3.0$ bar
$T_{LP} = 423.15$ K
$V_{tot} = 150000\ m^3$
$r_H = 0.05$
$2MW \le \dot{W}_{GT_n} \le 30MW$
$\dot{W}_{ST_{UB}} = 30$ MW

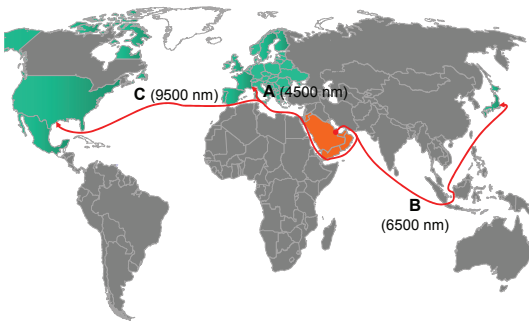

Figure 1. LNG trading routes.

where the (+) sign is valid for a minimization problem, while the (–) is valid for a maximization problem.

Logical constraints in Eqs. (6) and (7) have been also incorporated to the penalty term in a similar way. It must be noted that all constraints have been normalized, in order to have the same penalty impact.

The optimization problem has been solved in its time decomposed formulation as presented in Section 3.2. Two instances of the PSOStr algorithm have been used, one for the synthesis – design (Level A) and one for the operation (Level B) optimization problem.

The optimization problem is particularly demanding in terms of both computing time and solution stability and accuracy. For instance, a service speed of 21 kn and a sailing distance of 9500 nm result in 39 Level B problems to be solved in each Level A iteration. In addition, failure of the algorithm to converge (stochastic nature of the algorithm) in only one Level B problem will cause an instability (penalization of the candidate solution with no reason) to the Level A optimization procedure. In order to address these issues and improve both the stability and the execution time, the following measures have been taken during the problem set up:

a) In case that a Level B problem fails to converge, the problem is solved once more. Due to the stochastic nature of the algorithm, every execution starts with a new initial population. This has proved to be adequate to ensure 100% convergence success.
b) In order to reduce unnecessary Level B optimization execution, when a Level A candidate solution violates Level A constraints and the nominal power output is lower than the maximum power demand, Level B executions are not performed and the candidate solution is penalized accordingly.
c) Different sets of algorithmic parameters (population size and maximum generations) have been used, according to problem type and size. Parameter settings are presented in Table 2.

5. RESULTS

5.1 Solution of the Problem for the Longest Route (Route C)

The optimization problem has been solved with the numerical data in Table 1 of this paper and the energy demand profiles in Table 1 in Dimopoulos and Frangopoulos (2008a).

The optimal synthesis, design and operation of the system are depicted in Table 3. The total efficiency of the system per round-trip appearing in Table 3 is defined as follows:

$$\eta_{tot,rnd} = \frac{\sum_{t=1}^{N_T} \left(\dot{W}_{net} + \dot{Q}_D \right)_t \cdot \Delta\tau_t}{\sum_{t=1}^{N_T} \dot{m}_{fuel_{cons}} \cdot H_{u_{BOG}} \cdot \Delta\tau_t} \quad (24)$$

The optimum synthesis of the system consists of two gas turbines, each one feeding one dual pressure HRSG, and one extraction steam turbine. The gas turbines have nominal power outputs of 20.3 MW and 6.2 MW. The HRSGs produce HP steam of 24 bar and LP steam of 3 bar. The extraction steam turbine has a nominal power output of 10 MW.

TABLE 2. PSOStr parameter settings.

		Population	Generations
Level A		80	120
Level B	Phase		
	1 & 2 with $N_{GT} < 4$	60	350
	1 & 2 with $N_{GT} \geq 4$	60	500
	3	40	800
	4	40	800
	5	40	800

The optimal service speed is 21 kn, which results in a round-trip duration of 39.7 days. Full load and ballast voyage have each a duration of 18 days. During the full load voyage the gas turbine and steam turbine units operate near their nominal points with small adjustments to account for the variation in boil-off quantity and heating value. It is worth noting that during full load voyage the dual pressure HRSG units do not produce LP steam. LP steam demand is covered by the extraction in the steam turbine. In the ballast voyage, the GT unit with the high power output operates near its nominal point, while the small GT unit adjusts to the part load demand. In some of the ballast voyage time intervals (days), LP steam demand is also solely covered by the extraction in the steam turbine.

In both full load and ballast voyages the system requirements in BOG are significantly higher than the natural BOG. Therefore, BOG is supplemented by forced evaporation. BOG variation during full load and ballast voyages is depicted in Figs. 2 and 3.

In phases 3 and 4 of the round-trip, when the system uses MGO, the loads are covered by the small GT unit and the ST. The HRSG in operation produces both HP and LP steam, the last one being supplemented with extraction from the ST. In phase 5, both GT units are in operation, while only one HRSG is used to produce HP steam. LP steam demand is covered by extraction from the ST.

One would expect that the small number of time intervals with production of LP steam by the HRSG would lead the optimal synthesis optimization to single pressure HRSG units. However, dual pressure HRSG systems were selected. The reason for the existence of dual pressure HRSG is that the efficiency of HP steam production by a two-stage evaporation and pressure increase is significantly higher than the efficiency of the single pressure evaporation.

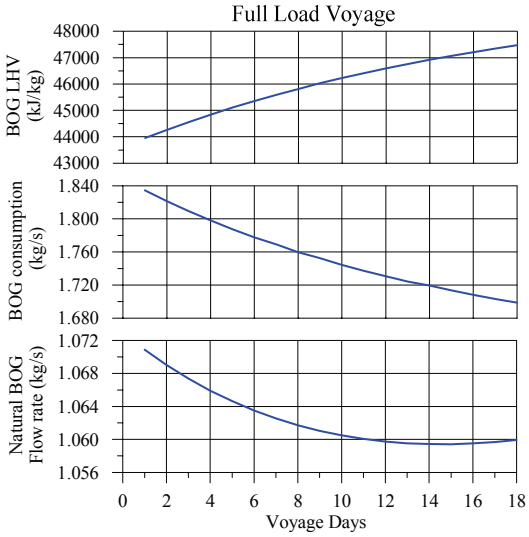

Figure 2. BOG Variation during full load voyage.

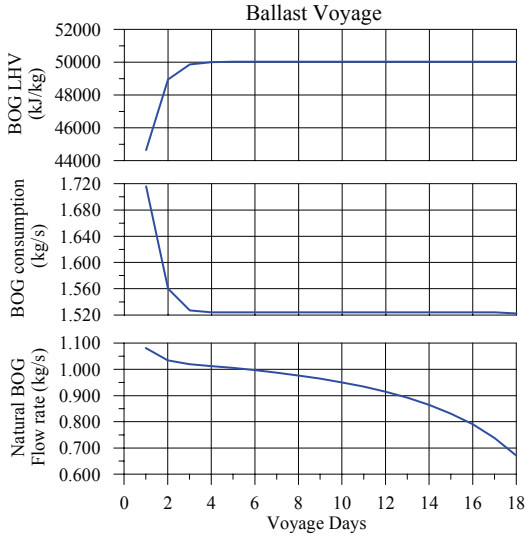

Figure 3. BOG variation during ballast voyage.

5.2 Solution of the Problem for Routes A and B

In order to study the effect of route selection, the optimization problem has been also solved for the other two typical trading routes. Optimal synthesis and design for all three routes are presented in Fig. 4 and Table 4. Due to space limitations, operation optimization results are not shown here.

The optimum NPV of the system increases significantly with shorter routes, because the number of round-trips per year increases and thus, the annual profits from delivering LNG increase. The higher profits in shorter routes allow for more complex optimum synthesis (higher installation costs) in order to cover the

TABLE 3. Optimization Results for Route C (S = 9500 nm)

Optimal Synthesis		Optimal Design		Optimization Results
N_{GTA}	1	V_S (kn)	21.00	Net Present Value: NPV^* = 810 x 10^6 US$
N_{GTB}	1	$\dot{W}_{GTA_n}$ (kW)	20323.28	Installation Cost: $C_{INST}{}^*$ = 20 x 10^6 US$
$I_{CONNECT}$	1	$\dot{W}_{GTB_n}$ (kW)	6195.54	Operating Costs: $C_{op,y}$ = 12.2 x 10^6 US$
I_{HRSG}	1 (2P)	P_{HP} (bar)	24.00	Operating Profit: F_y = 84.5 x 10^6 US$
I_{ST}	1	T_{HP} (K)	589.61	Round-Trip Duration: $_1\Delta\tau_{rnd}$ = 39.7 days
N_{GT} & N_{HRSG}	2 & 2	$\dot{W}_{ST_n}$ (kW)	9995.67	Round-Trips per year: N_{rnd} = 9.19 trips/year
				LNG Delivered: $V_{Deliverd}$ = 136357 m^3
				Total Efficiency: $\eta_{tot,rnd}$ = 0.5092
				(per round-trip)

Optimal Operation

Phase	Voyage Day	Gas Turbine Units (N_{GT} = 2)				HRSG Units (N_{HRSG} = 2)				ST Unit		$\dot{C}_{op}{}^*$
		$f_{L,GT1}$ (–)	$\dot{W}_{GT1}$ (kW)	$f_{L,GT2}$ (–)	$\dot{W}_{GT2}$ (kW)	f_{bp1} (–)	f_{LP1} (–)	f_{bp2} (–)	f_{LP2} (–)	f_{ext} (–)	$\dot{W}_{ST}$ (kW)	($ / h)
Full Load Voyage	1	1.0000	20323	0.9972	6178	0.9262	0.0000	1.0000	0.0000	0.1326	9996	1533.5
	2	1.0000	20323	0.9972	6178	1.0000	0.0000	0.7892	0.0000	0.1326	9996	1524.4
	3	1.0000	20323	0.9977	6181	1.0000	0.0000	0.7883	0.0000	0.1326	9993	1516.4
	4	0.9998	20319	0.9978	6182	1.0000	0.0000	0.7893	0.0000	0.1326	9996	1508.8
	5	0.9991	20306	1.0000	6196	0.9261	0.0000	1.0000	0.0000	0.1326	9996	1502.1
	6	1.0000	20323	0.9972	6178	1.0000	0.0000	0.7892	0.0000	0.1326	9996	1495.2
	7	1.0000	20323	1.0000	6196	1.0000	0.0000	0.7839	0.0000	0.1328	9978	1489.5
	8	0.9991	20306	1.0000	6196	1.0000	0.0000	0.7900	0.0000	0.1327	9996	1483.3
	9	1.0000	20323	1.0000	6196	1.0000	0.0000	0.7839	0.0000	0.1328	9978	1478.4
	10	1.0000	20323	0.9972	6178	0.9262	0.0000	1.0000	0.0000	0.1326	9996	1473.3
	11	0.9991	20306	1.0000	6196	0.9261	0.0000	1.0000	0.0000	0.1326	9996	1468.6
	12	0.9992	20306	1.0000	6196	1.0000	0.0000	0.7928	0.1443	0.1287	9995	1464.1
	13	0.9991	20306	1.0000	6196	1.0000	0.0000	0.7898	0.0000	0.1326	9996	1459.7
	14	1.0000	20323	1.0000	6196	1.0000	0.0000	0.7839	0.0000	0.1328	9978	1456.2
	15	1.0000	20323	0.9978	6182	1.0000	0.0000	0.7880	0.0000	0.1326	9992	1452.3
	16	0.9991	20306	1.0000	6196	0.9261	0.0000	1.0000	0.0000	0.1326	9996	1449.2
	17	1.0000	20323	0.9972	6178	1.0000	0.0000	0.7892	0.0000	0.1326	9996	1445.6
	18	1.0000	20323	0.9972	6178	1.0000	0.0000	0.7892	0.0000	0.1325	9996	1442.6
Ballast Voyage	1	1.0000	20323	0.7028	4354	1.0000	0.0000	1.0000	1.0000	0.0813	9910	1447.5
	2	1.0000	20323	0.7028	4354	1.0000	0.0000	1.0000	1.0000	0.0813	9910	1343.7
	3	1.0000	20323	0.6891	4269	0.9957	0.0000	1.0000	0.0000	0.1326	9996	1319.9
	4	1.0000	20323	0.6938	4299	1.0000	0.0000	1.0000	0.0000	0.1327	9967	1318.2
	5	1.0000	20323	0.7304	4525	1.0000	0.8975	1.0000	0.0000	0.0000	9741	1329.0
	6	1.0000	20323	0.7313	4531	1.0000	0.9131	1.0000	0.0000	0.0000	9731	1329.2
	7	1.0000	20323	0.7313	4531	1.0000	0.9131	1.0000	0.0000	0.0000	9731	1329.2
	8	1.0000	20323	0.7313	4531	1.0000	0.9131	1.0000	0.0000	0.0813	9710	1321.2
	9	1.0000	20323	0.7313	4531	1.0000	0.9131	1.0000	0.0000	0.0000	9731	1329.2
	10	1.0000	20323	0.7313	4531	1.0000	0.9131	1.0000	0.0000	0.0000	9731	1329.2
	11	1.0000	20323	0.7313	4531	1.0000	0.9131	1.0000	0.0000	0.0000	9731	1329.2
	12	1.0000	20323	0.7313	4531	1.0000	0.9131	1.0000	0.0000	0.0000	9731	1329.1
	13	1.0000	20323	0.7313	4531	1.0000	0.9131	1.0000	0.0000	0.0000	9731	1329.2
	14	1.0000	20323	0.7313	4531	1.0000	0.9131	1.0000	0.0000	0.0000	9731	1329.2
	15	1.0000	20323	0.7156	4434	1.0000	0.0000	0.9649	1.0000	0.0854	9830	1323.2
	16	1.0000	20323	0.7005	4340	1.0000	0.0000	0.9649	1.0000	0.0856	9924	1323.1
	17	1.0000	20323	0.6902	4276	1.0000	0.0000	0.9649	1.0000	0.1109	9970	1320.4
	18	1.0000	20323	0.6891	4269	0.9957	0.0000	1.0000	1.0000	0.1326	9996	1316.6
Maneuvering		0.0000	0	0.8406	5208	0.0000	0.0000	1.0000	1.0000	0.0000	1136	891.9
Loading		0.0000	0	0.6559	4063	0.0000	0.0000	1.0000	1.0000	0.2291	1043	756.1
Off loading		0.2000	4065	0.9928	6151	0.0000	0.0000	0.9896	0.0000	0.4450	1782	1764.1

[1] Additional nomenclature are presented in the accompanying papers (Dimopoulos and Frangopoulos 2008a, b).

system loads in each phase of operation more efficiently. In addition, the service speed also increases.

The results presented in Table 4 for the three routes are obtained with the same values of all the other parameters (except the distance). In real LNG vessel operation, both CIF and FOB values, which are contractually determined, also vary with route selection and tend to decrease with shorter routes. Therefore, real profits of the system in shorter routes are also expected to be lower than the values presented here. Nevertheless, these results reveal the basic trends of optimal system configuration for shorter routes. It is worth noting, that in most cases the trading route is determined during the early specification phase of a LNG vessel construction, since LNG shipping involves long

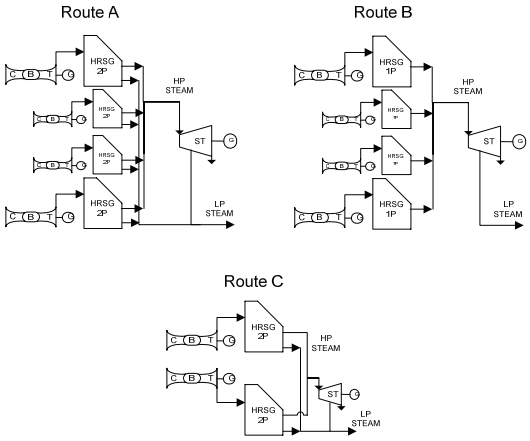

Figure 4. Optimum system synthesis in each of the three routes.

TABLE 4. Optimization results for the COGES system for three different trading routes.

Route A: S = 4500 nm				
Optimal Synthesis		Optimal Design		Optimization Results
N_{GTA}	2	V_S (kn)	23.00	Net Present Value: $NPV^* = 1931 \times 10^6$ US$
N_{GTB}	1	$\dot{W}_{GTA_n}$ (kW)	17692.79	Installation Cost: $C_{INST}^* = 29 \times 10^6$ US$
$I_{CONNECT}$	1	$\dot{W}_{GTB_n}$ (kW)	2000.00	Operating Costs: $C_{op,y} = 17.6 \times 10^6$ US$
I_{BOILER}	1 (2P)	P_{HP} (bar)	31.34	Operating Profit: $F_y = 199.6 \times 10^6$ US$
I_{ST}	1	T_{HP} (K)	635.22	Round-Trip Duration: $\Delta\tau_{rnd} = 18.3$ days
N_{GT} & N_{HRSG}	4 & 4	$\dot{W}_{ST_n}$ (kW)	15331.34	Round-Trips per year: $N_{rnd} = 19.94$ trips / year
				LNG Delivered: $V_{Deliverd} = 138493$ m^3
				Total Efficiency: $\eta_{tot,rnd} = 0.4902$ (per round-trip)
Route B: S = 6500 nm				
Optimal Synthesis		Optimal Design		Optimization Results
N_{GTA}	2	V_S (kn)	23.00	Net Present Value: $NPV^* = 1280 \times 10^6$ US$
N_{GTB}	1	$\dot{W}_{GTA_n}$ (kW)	18108.39	Installation Cost: $C_{INST}^* = 27 \times 10^6$ US$
$I_{CONNECT}$	1	$\dot{W}_{GTB_n}$ (kW)	2000.00	Operating Costs: $C_{op,y} = 17.9 \times 10^6$ US$
I_{BOILER}	0 (1P)	P_{HP} (bar)	50.00	Operating Profit: $F_y = 133.1 \times 10^6$ US$
I_{ST}	1	T_{HP} (K)	703.52	Round-Trip Duration: $\Delta\tau_{rnd} = 25.6$ days
N_{GT} & N_{HRSG}	4 & 4	$\dot{W}_{ST_n}$ (kW)	15411.65	Round-Trips per year: $N_{rnd} = 14.29$ trips / year
				LNG Delivered: $V_{Deliverd} = 136627$ m^3
				Total Efficiency: $\eta_{tot,rnd} = 0.4800$ (per round-trip)
Route C: S = 9500 nm				
Optimal Synthesis		Optimal Design		Optimization Results
N_{GTA}	1	V_S (kn)	21.00	Net Present Value: $NPV^* = 810 \times 10^6$ US$
N_{GTB}	1	$\dot{W}_{GTA_n}$ (kW)	20323.28	Installation Cost: $C_{INST}^* = 20 \times 10^6$ US$
$I_{CONNECT}$	1	$\dot{W}_{GTB_n}$ (kW)	6195.54	Operating Costs: $C_{op,y} = 12.2 \times 10^6$ US$
I_{BOILER}	1 (2P)	P_{HP} (bar)	24.00	Operating Profit: $F_y = 84.5 \times 10^6$ US$
I_{ST}	1	T_{HP} (K)	589.61	Round-Trip Duration: $\Delta\tau_{rnd} = 39.7$ days
N_{GT} & N_{HRSG}	2 & 2	$\dot{W}_{ST_n}$ (kW)	9995.67	Round-Trips per year: $N_{rnd} = 9.19$ trips / year
				LNG Delivered: $V_{Deliverd} = 136357$ m^3
				Total Efficiency: $\eta_{tot,rnd} = 0.5092$ (per round-trip)

time chartering agreements between fixed loading and off-loading locations. Therefore, the sailing distance (trading route) is usually a parameter of the optimization problem. The effect of trading routes changing during the lifetime of the vessel on the optimal system could be a subject of further investigation.

6. CONCLUSIONS

The synthesis, design and operation optimization of the marine COGES energy system for a LNG vessel has been investigated in this study. Detailed modeling of both the energy system components and the LNG boil-off process has been applied to accurately assess the thermoeconomic behavior of the system. The time decomposition approach has been capable of accurately handling the time dependency of this problem.

In addition, it has been revealed that the trading route has a significant impact on both the optimum synthesis and the design service speed of the system.

NOMENCLATURE[1]

I	Logical variable
i_r	Market interest rate [–]
N	Number of components
N_e	Period of economic analysis [years]
N_T	Number of time intervals
NPV	Net Present Value [US $]
w	Synthesis optimization independent variables
x	Operation optimization independent variables
z	Design optimization independent variables

Greek Letters

$\Delta\tau$	Duration of time interval [h]
ϕ	Installation cost factor

Subscripts

LB	Lower bound
t	Time increment
UB	Upper bound

Superscripts

*	Optimum

REFERENCES

Andrianos, K., 2006, "Techno-economic Evaluation of various Energy Systems for LNG carriers", Diploma Thesis, National Technical University of Athens, Athens, Greece.

BunkerWorld, 2007, "Marine Fuel Prices, Historical Data".

Dimopoulos, G. G., 2007, "Mixed-variable engineering optimization based on evolutionary and social metaphors", *Computer Methods in Applied Mechanics and Engineering,* Vol. 196, No. 4-6, pp. 803-817.

Dimopoulos, G. G., and C. A. Frangopoulos, 2006, "Optimization of Energy Systems Based on Evolutionary and Social Metaphors", *Proceedings of The 19th International Conference on Efficiency, Cost, Optimization, Simulation and Environmental Impact of Energy Systems (ECOS).* C. A. Frangopoulos, et al., Vol. 1, pp. 523-532.

Dimopoulos, G. G., and C. A. Frangopoulos, 2008a, "A dynamic model for liquefied natural gas evaporation during marine transportation", *International Journal of Thermodynamic*, Vol. 11, No. 3, pp.123-132.

Dimopoulos, G. G. and C. A. Frangopoulos, 2008b, "Thermoeconomic simulation of marine energy systems for a Liquefied Natural Gas carrier", *International Journal of Thermodynamics,*Vol. 11, No. 4, pp. 195-201.

Dimopoulos, G. G., A. Kougioufas, V. and C. A. Frangopoulos, 2006, "Synthesis, Design and Operation Optimization of a Marine Energy System", *Proceedings of Proceedings of The 19th International Conference on Efficiency, Cost, Optimization, Simulation and Environmental Impact of Energy Systems (ECOS).* C. A. Frangopoulos, et al., Vol. 1, pp. 533-542.

Grueninger, T., and D. Wallace, 1996, "Multi-modal optimization using genetic algorithms", MIT CADlab - Technical Report 96.02, Massachusetts Institute of Technology, Cambridge MA.

Kennedy, J., Y. Shi and R. C. Eberhart, 2001, *Swarm* intelligence*,* Morgan Kaufmann, San Francisco, CA.

Levander, O. and S. Hannula, 2004, "More gas for LNG carriers", *Wartsila Marine News,* Vol. 3, pp. 6-11.

MAN-B&W, 2004, "LNG Carrier Propulsion by ME-GI Engines and/or Reliquefaction", MAN Diesel SE.